Available online at www.sciencedirect.com
SCIENCE DIRECT
Solid State Ionics 177 (2006) 37 – 43
SOLID STATE IONICS
www.elsevier.com/locate/ssi

Infrared spectroscopy of superionic conductor $LiNaSO_4$: Vibrational modes and thermodynamics

Ming Zhang [a,*], Andrew Putnis [b], Ekhard K.H. Salje [a]

[a] Department of Earth Sciences, University of Cambridge, Downing Street, Cambridge, CB2 3EQ, UK
[b] Institut für Mineralogie, Westfälische Wilhelms-Universität Münster, Corrensstrasse 24, D-48149 Münster, Germany

Received 13 December 2004; accepted 5 October 2005

Abstract

Infrared active phonon spectra of lithium sodium sulphate, $LiNaSO_4$, were studied at temperatures between 20 K and 780 K. Dielectric constant [$\varepsilon=\varepsilon'+i\varepsilon''$] and energy loss function [$-\mathrm{Im}(1/\varepsilon)$] were obtained from Kramers–Kronig analysis. Our IR data show a more complete set of vibrational modes than previous investigations. The IR data of $LiNaSO_4$ at 20 K are consistent with the $P31c$ symmetry, indicating that $LiNaSO_4$ shows no structural phase transitions between 20 K and 300 K, in contrast to $LiKSO_4$. On heating from 20 K, phonon modes related to Li and Na vibrations show a dramatic line broadening and decrease in intensity. An extra mode is recorded near 380 cm^{-1} at 500 K. The absorption shows a systematic increase in intensity on further heating. These changes are attributed to anharmonic effects and Li diffusion or hopping. Dramatic spectral changes in the internal modes occur near 620 K on heating, suggesting the onset of the rotational disorder of SO_4 tetrahedra, but the Li atom spectrum shows weak response to the rotational disorder.

Keywords: $LiNaO_4$; Infrared spectroscopy; Dielectric constant; Transverse and longitudinal optical mode; Li disorder; Ionic conductivity

1. Introduction

Lithium sodium sulphate, $LiNaSO_4$, belongs to the family of mixed sulphates of the $LiMSO_4$ (M=Na, K, Rb, NH_4, Ag) type, which exhibits interesting properties of ionic conduction. The room temperature structure of $LiNaSO_4$ is believed to belong to space group $P31c$ (C_{3v}^4) with six molecules in the hexagonal cell (unit cell parameter $a_0=7.627$ Å and $c=9.8579$ Å; and density=2.527 $g\cdot cm^{-3}$) [1]. On heating, $LiNaSO_4$ undergoes a phase transition near 791 K (from the room-temperature trigonal symmetry to a body centre cubic symmetry) [2–4], with a dramatic increase in volume (by 6%) [5] and ionic conductivity [6–8]. ^7Li and ^{23}Na nuclear magnetic resonance (NMR) analysis shows increasing Li and Na diffusion on heating [9–11].

Although optical properties of $LiNaSO_4$ have been the subject of several previous investigations [12–17], some important issues remain unclear. First, the number of optical phonon modes of the material revealed previously by vibrational spectroscopy was far fewer than the predicted modes. While diffraction measurements indicate that the material has the group space of $P31c$ at room temperature [1], only two of the six expected v_2 modes (SO_4) were observed. Questions related to the structure of $LiNaSO_4$ were also put forward by other studies. NMR results of Junke et al. [18], which reported 12 different electric field gradient tensors inconsistent with the $P31c$ space group, seem to contradict the results of Morosin and Smith [1]. Second, the mechanism of ionic conduction in the high-temperature phases of $LiNaSO_4$ and other related compounds has been a subject of discussion [3,19–24]. Various models (e.g., the combination of the paddle wheel and percolation models) were proposed for the high-temperature ionic conductivity of $LiNaSO_4$, while there is a lack of clear evidence to clarify the different mechanisms.

The aims of this study are, first, we wished to gain a better understanding of the optical phonons of $LiNaSO_4$. This includes revealing the previously unobserved SO_4 modes. In the present study, dielectric properties of the crystal [e.g., dielectric constant $\varepsilon(\omega)=\varepsilon'(\omega)+i\varepsilon''(\omega)$, dielectric loss $=-\mathrm{Im}(1/\varepsilon)=\varepsilon''/(\varepsilon'^2+\varepsilon''^2)$, and optical conductivity $\sigma(\omega)=(\omega/4\pi)\mathrm{Im}(\varepsilon)$] were extracted from infrared reflectance data after

* Corresponding author. Tel.: +44 1223 333411; fax: +44 1223 333450.
E-mail address: mz10001@esc.cam.ac.uk (M. Zhang).

0167-2738/$ - see front matter © 2005 Elsevier B.V. All rights reserved.
doi:10.1016/j.ssi.2005.10.001

Kramers–Kronig analysis in order to identify the TO-LO (transverse optical–longitudinal optical modes) splitting of infrared active phonons. The LO modes of $LiNaSO_4$ have not been fully identified previously, in spite of several previous Raman and IR studies on $LiNaSO_4$. Second, we focused on the thermal dynamics of $LiNaSO_4$, especially the possible influence of Li disorder on the phonon behaviour of $LiNaSO_4$ or the potential coupling between Li modes and the internal modes of the SO_4 group. This may lead to a better understanding of the structure changes at the atomic level and the ionic conductivity of $LiNaSO_4$.

2. Experimental

The $LiNaSO_4$ crystals were grown by slow evaporation of aqueous solution. The structures of the crystals at room temperature were confirmed by powder X-ray diffraction analysis. For polarized single crystal reflectance measurements, the crystallographic orientations of the crystals were determined from the external morphology. Conventional infrared powder technique [25] was used for the measurements at high and low temperatures. Polyethylene, cesium iodide and potassium bromide powders and 0.5-mm double-polished Si wafers [26] were used as matrix materials or substrates for the IR measurements.

Using a Bruker 113v FT-IR spectrometer, the reflection and absorption spectra at temperatures between 20 K and 780 K were recorded under vacuum to avoid absorption from water and carbon oxides in the air. Experiments were performed in both the mid-infrared, in the region of 500–1500 cm^{-1} using an HgCdTe detector cooled with liquid nitrogen, and the far-infrared, the region of 20–700 cm^{-1} using a room-temperature DTGS detector. Instrumental resolution of 0.4 and 2 cm^{-1} was used between 300 and 1500 cm^{-1} and 2 cm^{-1} between 50 and 350 cm^{-1}. Gold mirrors and a KRS5 polarizor were used for the polarized reflectance measurements. For heating experiments, the samples were placed in a cylindrical platinum-wound furnace in the spectrometer's sample chamber. Temperatures were allowed to stabilize for 15 min between collections and were measured using a Pt/PtRh thermocouple placed against the samples. A close cycle liquid-helium cryostat (LEYBOLD), equipped with KRS5 and polyethylene windows, was used for low-temperature experiments. Absorption spectra were calculated by measuring sample and reference beam spectra collected at the same temperatures.

3. Results

3.1. Infrared spectrum of $LiNaSO_4$ and band assignments

$LiNaSO_4$ is trigonal with space group $P31c$. By group theory, the irreducible representations of the internal and external optical modes are [14]

$$\text{Internal modes of the } SO_4: \ \Gamma_{\text{int}} = 9A_1 + 9A_2 + 18E \quad (1)$$

$$\text{External modes}: \ \Gamma_{\text{ext}} = 11A_1 + 12A_2 + 23E \quad (2)$$

A_1 and E modes are both infrared and Raman active, whereas the A_2 modes are optically inactive. The A_1 modes can be seen in IR spectra when the electric vector of the incident infrared radiation, $\boldsymbol{E}$, is perpendicular to the c-axis while the E modes can be observed when the $\boldsymbol{E}$ is parallel to the c-axis. The optical modes of $LiNaSO_4$ can be classified into two different groups: the internal modes of SO_4 group and the external modes associated with translational/rotational and cation vibrations. Among the internal modes, there are three v_1 modes ($3A_1$), six v_2 modes ($6E$), nine v_3 ($3A_1+6E$) and nine v_4 modes ($3A_1+6E$). The v_1 and v_3 modes indicate the symmetric and anti-symmetric stretching vibrations of the SO_4, respectively. The v_2 and v_4 modes are associated with the symmetric and anti-symmetric bending vibrations of the SO_4, respectively. Among the predicted external modes, 12 phonon modes are expected to be mainly associated with Li or ion motions ($3A_1+3A_2+6E$), and only nine ($3A_1+6E$) of them are optically active. These external modes are located in the far-IR region.

Polarized IR reflectance spectra of A_1 and E species of $LiNaSO_4$ are shown in Fig. 1. One of the important features in the reflectance spectrum of $LiNaSO_4$ is the significant increase in reflectivity with decreasing wavenumber in the far-IR region. As is commonly seen in materials with high conductivities (such as high-T_c superconductors and superionic conductors) [27,28], this behaviour indicates that $LiNaSO_4$ possesses high optical conductivity [optical conductivity $\sigma(\omega)=(\omega/4\pi)\mathrm{Im}(\varepsilon)$]. The dielectric function [$\varepsilon(\omega)=\varepsilon'(\omega)+i\varepsilon''(\omega)$] and dielectric loss [$-\mathrm{Im}(1/\varepsilon)=\varepsilon''/(\varepsilon'^2+\varepsilon''^2)$] (Fig. 2) were obtained through Kramers–Kronig analysis of the measured reflection spectra (Fig. 2a–c). The accuracy of the experimental data was checked using the sum rule [29]:

$$\int_0^{\omega_o} \frac{\varepsilon''(\omega)}{\omega} \mathrm{d}\omega = \frac{\pi}{2}(\varepsilon_o - \varepsilon_\infty) \quad (3)$$

where ε_o and ε_∞ are the static and high-frequency dielectric constants, respectively, while ω_o is a frequency which is high enough to include all vibrational modes in the integral. The integration was performed between 20 and 5000 cm^{-1}. The left-hand side of expression (3) gives values of 4.92 ($\boldsymbol{E} \perp c$) and

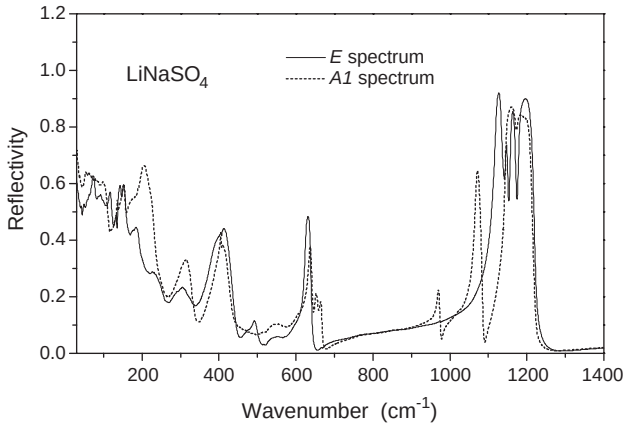

Fig. 1. Polarized reflectance spectra (30–1400 cm^{-1}) of $LiNaSO_4$. The A_1 spectrum was obtained with $\boldsymbol{E}$, the incident infrared radiation, perpendicular to the c-axis, whereas the $\boldsymbol{E}$ spectrum was recorded with E parallel to the c-axis.

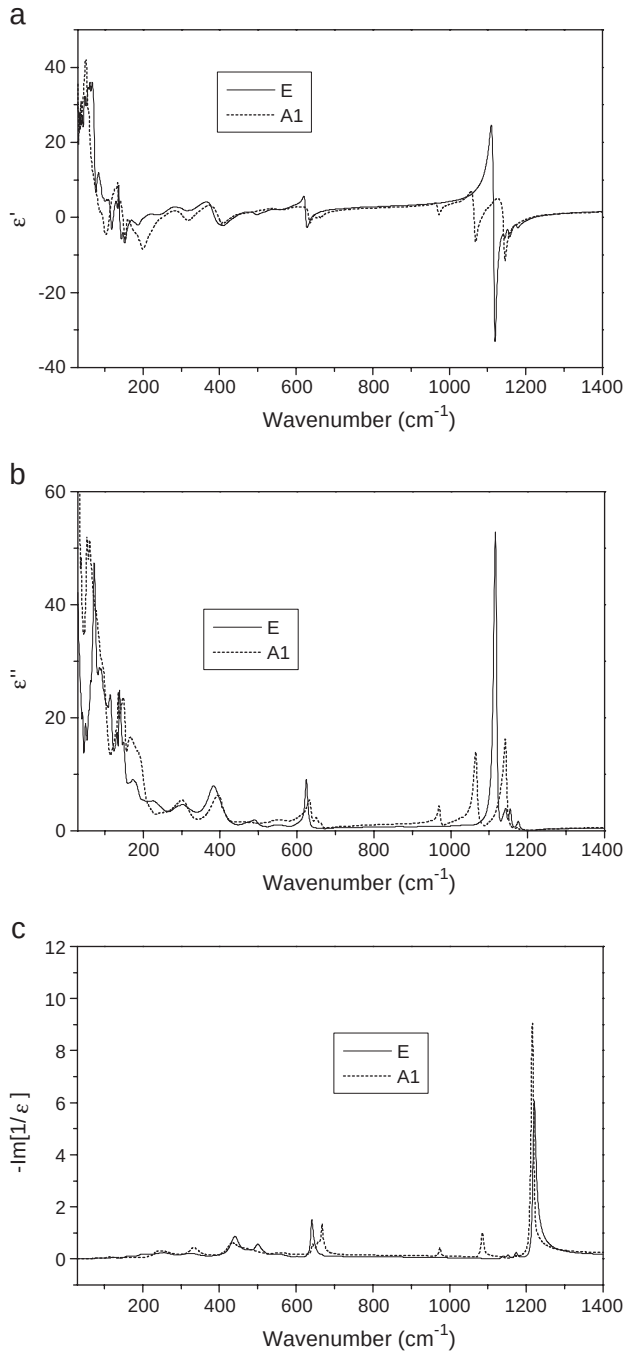

Fig. 2. (a) Real part of the dielectric constant; (b) imaginary part of dielectric constant; and (c) energy loss function.

5.21 ($\boldsymbol{E} \parallel c$) in agreement with $\pi(\varepsilon_o - \varepsilon_\infty)/2 = 4.41$ with $\varepsilon_o = 5.0$ [17] and $\varepsilon_\infty = 2.2$ [30]. This indicates that the reflectance measurements and Kramers–Kronig analysis yield reliable absolute data. The frequency of TO phonons are given by peak positions in ε'' while LO phonon frequencies can be obtained from the maxima of the dielectric loss function, $-\mathrm{Im}(1/\varepsilon) = \varepsilon''/(\varepsilon'^2 + \varepsilon''^2)$. The observed TO and LO modes for both A_1 and E species are listed in Table 1. Our data are consistent with previous work [13,17] which identified some of the modes. Here, we report additional optical modes (especially some of the previously unresolved bending modes of SO_4).

Table 1
Frequencies (in cm^{-1}) of infrared modes of $LiNaSO_4$

Internal modes	A_1 modes		E modes		Assignment
	TO	LO	TO	LO	
v_1	970	974			Symmetric stretching
($3A_1$)	998	1002			of SO_4
	1026	1026			
v_2			470	(at 20 K)	Symmetric bending
($6E$)			481	(at 20 K)	of SO_4
			486	(at 20 K)	
			490	501	
			514	(at 20 K)	
v_3	1065	1086	1116	1140	Anti-symmetric
($3A_1+6E$)	1142	1173	1142	1152	stretching of SO_4
	1171	1215	1154	1172	
			1175	1220	
v_4	632	643	617	(at 20 K)	Anti-symmetric
($3A_1+6E$)	651	657	619	(at 20 K)	bending of SO_4
	662	667	624	641	
			637	(at 20 K)	
			646	(at 20 K)	
			665	666	

External	A_1 modes		Assignment	E modes		Assignment
	TO	LO		TO	LO	
	396	432	Li mode	382	440	Li mode
	300	332	Li mode	302	329	Li mode
	184	194		290		Li mode
	164			228	255	
	148	157		176	204	
	90	113		138	145	
	60			114	123	
				88	106	

TO = transverse optical mode, and LO = longitudinal optical mode.

The internal modes of the SO_4 ions occur as well-separated groups in IR and Raman spectra [31] and are separated from external modes (Figs. 3 and 4). The v_1 modes (A_1, symmetric stretching of SO_4) are commonly located in a wavenumber

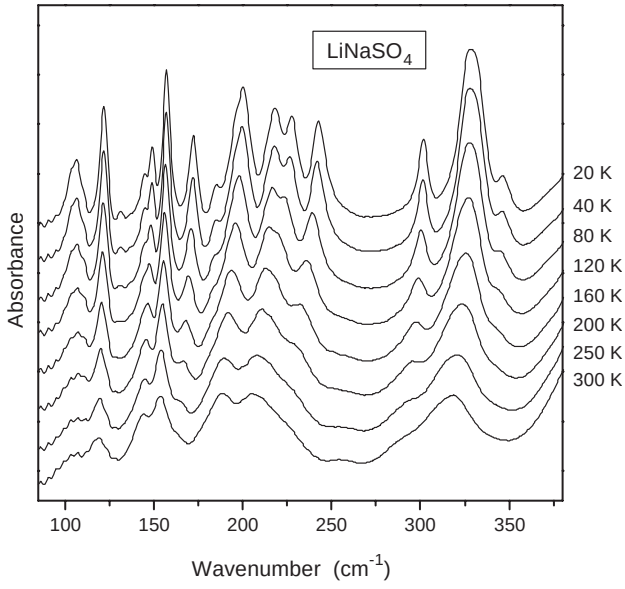

Fig. 3. Temperature evolution of absorption spectrum (85–380 cm^{-1}) of $LiNaSO_4$ between 20 K and 300 K.

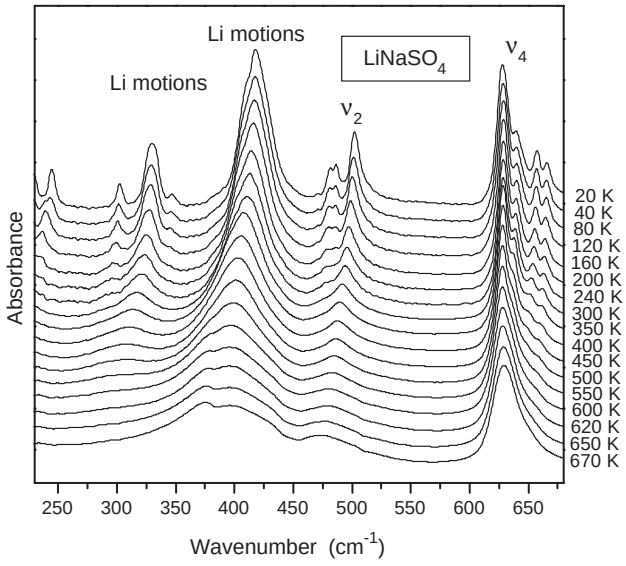

Fig. 4. Temperature evolution of absorption spectrum (230–680 cm^{-1}) of $LiNaSO_4$ between 20 K and 670 K. An additional Li mode near 380 cm^{-1} occurs near 500 K.

range lower than those of the v_3 modes, and they have weak intensity. The predicted three v_1 of the SO_4 were detected at 970, 988 and 1026 cm^{-1} (TO frequency) (Table 1). These v_1 modes exhibit little TO-LO splitting (Fig. 2b and c). For instance, the two TO modes near 970 and 988 cm^{-1} give rise to a frequency splitting of only 4 cm^{-1}, while the 1026 cm^{-1} mode shows almost no splitting. The observed small TO-LO splitting for the v_1 modes in $LiNaSO_4$ is consistent with the similar observation from other lithium sulphates [30]. Our spectrum (with $\boldsymbol{E} \perp c$) revealed all three predicted v_3 modes (at 1065, 1142 and 1171 cm^{-1}) with A_1 symmetry. These v_3 modes (anti-symmetric stretching of the SO_4) show a relatively large LO-TO splitting (about 30 cm^{-1}), in contrast to those (a few cm^{-1}) of the v_1 modes (Fig. 2b and c). We observed four of the six anti-symmetric stretching modes with E symmetry (Table 1). The missing two modes are expected to have very low intensity.

The six predicted v_2 modes (symmetric bending) of the SO_4 all belong to the E species. Our reflectance data obtained at room temperature revealed only one of them near 490 cm^{-1} (Fig. 2b, Table 1). Powder absorption measurements at 20 K revealed four other modes at 470, 481, 486 and 514 cm^{-1}. Some of them showed very weak intensities (Fig. 4). As described earlier, the v_4 modes (anti-symmetric bending) of the SO_4 consist of three A_1 and six E species and they were all revealed in the present study. The three A_1 v_4 modes were recorded at 632, 651 and 662 cm^{-1}, with LO frequencies of 643, 657 and 667 cm^{-1}, respectively. The other modes in the wavenumber range should be due to the v_4 modes with E symmetry. Our reflectance data show two modes (at 624 and 665 cm^{-1}) with $\boldsymbol{E} \parallel c$. In fact, the v_4 modes of $LiNaSO_4$ are situated so close to each other that they could be resolved only with high instrumental resolutions at low temperatures. Powder absorption spectra recorded with an instrumental resolution of 0.4 cm^{-1} at 20 K reveal additional modes at 617, 619, 637 and 646 cm^{-1} (Fig. 5). They are assigned as the other v_4 modes (E), which are missing in the room-temperature reflectance data.

The external modes are expected to be located in the far-IR region (Figs. 1, 3 and 4)). Similar to other sulphates [32–34], they consist of Li and Na translation vibrations as well as the rotational and translational modes of SO_4. The modes near 300 and 396 (A_1 symmetry) and those near 290, 302 and 384 (with E symmetry) are mainly attributed to Li motions. They showed strong frequency shift in ^6Li and ^7Li isotope substitutions [13]. We attribute most of the modes between 200 and 250 cm^{-1} to vibrations associated with Na motions, because their frequencies are consistent with the effect of the mass change between Na and Li, and also because they showed similar spectral changes (especially frequency shifts) as the Li modes during heating or cooling. The other modes in the far-IR region, which show a much weaker temperature dependence on cooling in contrast to these Li or Na modes (Fig. 3), could be due to rotations and translations associated with the SO_4. The external modes generally show a larger LO-TO splitting (about ~6–13%) (Table 1), in contrast to those (0–3%) of the internal modes.

3.2. Temperature dependence of infrared spectra

The change of sample temperature has different effects on the internal modes of the SO_4 and the Li modes. The data between 300 and 450 cm^{-1} (Figs. 3 and 4) show anomalous variations related to the Li modes. With increasing temperature, the Li modes at 330 and 418 cm^{-1} (values at 20 K) exhibit a pronounced broadening and a decrease in frequency and intensity (Fig. 4). The 418 cm^{-1} mode, which is the most intense signal among the Li modes, shifted to 392 cm^{-1} (a change of 6.22%) at 670 K. The Li mode near 330 cm^{-1} (at 20 K) moved to 292 cm^{-1} (a change of ~11.5%) at 600 K and

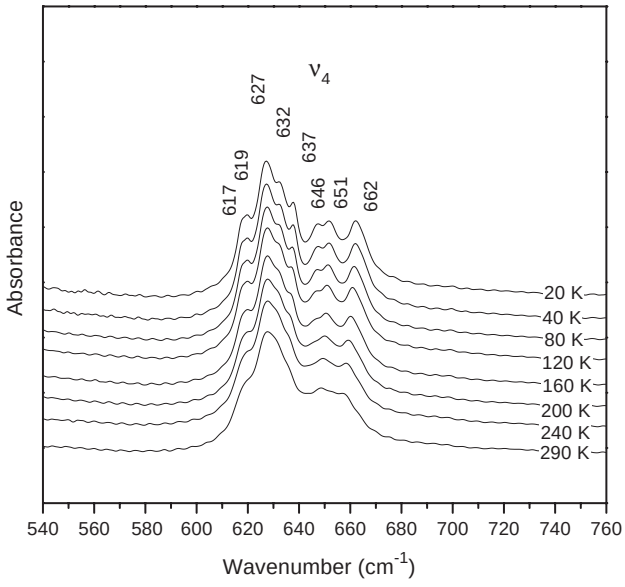

Fig. 5. The v_4 modes of the SO_4 measured at low temperatures with a high instrumental resolution (0.4 cm^{-1}).

became almost unresolvable above this temperature. We noted that an extra mode near 380 cm^{-1} appeared near 500 K and its intensity increased with further increasing temperature (Fig. 4). These changes are likely to be associated with the thermally induced Li diffusion or disorder as its frequency is in the spectral region where Li modes are located. In IR reflectance measurements, Pimenta et al. [17] recorded an additional mode at 385 cm^{-1} at temperature above the trigonal–cubic phase transition and it was attributed to Li motion. Our absorption measurements apparently had better resolution and revealed the feature at much lower temperatures. A similar extra mode at the similar wavenumber, whose intensity increased on heating, was also reported in the superionic conductor β-eucryptite ($LiAlSiO_4$) above 700 K [28]. The modes between 100 and 180 cm^{-1} also showed significant frequency shifts with changing temperature. For instance, the modes near 121 and 157 cm^{-1} (at 20 K) shifted to 119 and 153 cm^{-1} (with changes of 1.67% and 2.55%) at 300 K, respectively. Unfortunately, we could not measure high-temperature IR data between 80 and 250 cm^{-1} because polyethylene melts near 370 K. One can estimate that the change for these modes at 600 K could be around 3–5%.

The internal bands of the SO_4 show much weaker temperature dependences, in contrast to the strong spectral changes of the Li modes. The modes (v_1 and v_3) associated with S–O stretching vibrations generally indicate a very small change of frequency (0 to 2 cm^{-1}) between 20 K and 300 K, apart from slightly line narrowing (2–3 cm^{-1}). We also did not observe additional v_1 and v_3 modes at low temperatures. On heating the sample from 300 K to 570 K, the most intense v_1 mode near 970 cm^{-1} shows a very small decrease (only 0.5 cm^{-1}) in frequency (Fig. 7a). The mode exhibits a dramatic broadening on heating above 570 K, accompanied by a significant decrease in band height (Fig. 6). It eventually became a broad local maximum at higher temperatures. Similar variations were also recorded for the v_3 modes (Fig. 6). For instance, the v_3 mode near 1065 cm^{-1} (at 300 K) showed a thermal behaviour similar to that of the v_1 mode near 970 cm^{-1} (Fig. 6). On heating to 570 K, it exhibits a small decrease in frequency (2 cm^{-1}). It became a weak shoulder in the spectra recorded at 620 K and 650 K. On further heating, it was almost unresolvable. These changes are attributed to the orientational disorder of the SO_4 anions. In comparing IR data from $LiNaSO_4$ and $Li_2B_4O_7$ (it also has high ionic conductivity), we note that two materials show different spectral behaviour at high temperatures. Previously reported spectral data from $Li_2B_4O_7$ showed that although Li modes change dramatically on heating, IR modes associated with the framework of BO_4 and BO_3 anions exhibit no significant variations and there were no clear indications of rotation disorder of BO_4 and BO_3 [35].

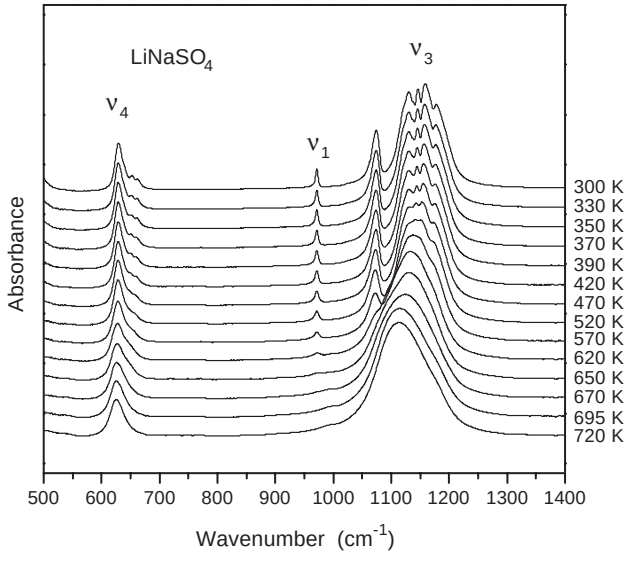

Fig. 6. Absorption spectra (500–1400 cm^{-1}) of $LiNaSO_4$ between 300 and 720 K.

4. Discussion

In comparison with our previous IR results of $LiKSO_4$ between 1.5 and 300 K [34], which showed sequential phase transitions associated with the different local configurations of the SO_4, we found some similarities between the temperature evolution of the far-IR spectra of $LiNaSO_4$ and $LiKSO_4$. For instance, more IR modes appeared on cooling in the region of 250 and 500 cm^{-1}, where the Li modes and the v_2 modes are located for both materials. What are the implications of these similarities? Does $LiNaSO_4$, like $LiKSO_4$, also undergo structural phase transitions? If not, what are the possible causes for the changes in $LiNaSO_4$? Our low-temperature data on $LiNaSO_4$ do not support the idea that there is a symmetry-breaking phase transition associated with variations or rotations of the SO_4 groups at low temperatures. In fact, the spectra remain consistent with the $P31c$ symmetry, in terms of the number of internal modes of SO_4. For instance, at 20 K, five v_2 modes and nine v_4 modes were detected and they are consistent with the predicted six v_2 and nine v_4 modes with consideration that the missing v_2 mode is too weak or overlay with other modes. More importantly, unlike $LiKSO_4$, $LiNaSO_4$ does not show the appearance of any additional modes or mode splitting for the v_1 and v_3 modes even at 20 K, which is a direct consequence of symmetry change of SO_4 sites in $LiKSO_4$ at low temperatures [34].

We now discuss the thermal behaviour of Li and SO_4 ions separately, in order to identify changes of transport mechanism in $LiNaSO_4$. Among all the vibrational modes observed, the modes related to Li (as well as Na) vibrations showed the strongest frequency shift (6–11% between 20 K and 600 K) and intensity and width variations. The Li mode near 330 cm^{-1} (at 20 K) almost vanished at 600 K, a temperature far below 788 K at which the phase transition (from trigonal to body centre cubic symmetry) takes place [3,4]. We attribute the thermal behaviour of Li modes to thermally induced Li diffusion or Li disorder which has been seen in $LiNaSO_4$ [10,11], other lithium sulphates [12,14] and other ionic conductors (e.g., β-eucryptite $LiAlSiO_4$) [36]. We associate the increase in a peak width (or damping) with a self-diffusion process of the element involved in the vibrational mode [37]. On heating, the dramatic increase in widths of Li bands is

consistent with the thermally enhanced Li diffusion revealed by NMR analysis [9–11].

As described earlier, we noted that the different types of the internal modes of SO_4 do not show the same thermal behaviour. For instance, the v_2 modes become gradually broader and weaker in intensity on heating from 20 K to room temperature, while the v_1 and v_3 modes show a very weak change between 20 K and 300 K. The differences are shown most in the width of individual modes as the widths for the v_3 modes show an insignificant increase on heating from 20 to 450 K, in contrast to the v_2 modes. In order to have a better comparison of this behaviour, the autocorrelation method [38] was used to extract the "width" of different features because of the difficulty in tracing individual modes of the overlaid Li and v_2 features that become very broad and weak at high temperatures. The analysis quantifies the relative change in band width of the absorption profile by the autocorrelation function Corr(g,t) [39]. The method has the advantage of giving a statistical measure proportional to the widths of the phonon modes. In addition, it can be used for those regions of the absorption spectra where curve-fitting analysis is difficult or impossible due to broad phonon absorption or mode overlaying. The data of the autocorrelation analysis on the Li, v_2 and v_3 features (in the regions of 265–465, 465–580 and 1025–1270 cm^{-1}, respectively) are plotted in Fig. 7. The results show that the change of temperature has a stronger effect on the v_2 modes than the v_3 modes. It is surprising that between 20 and 450 K, the variation associated with the broadening of the v_2 modes is more similar to that of the Li modes. This anomalous behaviour of the v_2 modes (especially the modes with the lowest frequency) could be related to the coupling between Li modes and v_2 modes, which are closest in the frequency spectrum. Similar coupling between Li modes and v_2 modes has been reported in $LiKSO_4$ [40,41]. However, this explanation is contradictory to the thermal behaviour of the other internal modes (v_1, v_3 and v_4) of SO_4, which apparently show temperature dependences different from the Li modes (Fig. 7).

We now focus on the ionic conductivity of $LiNaSO_4$ at high temperatures. The classic picture of ionic conductivity involves the jumping of ions between vacancies in the lattice or hopping of the ion out of one energy well or site into a nearby site. This means that high conductivities are associated with low activation energies that may consist of different contributions. Factors such as ion size, the valence state of the ion or cation, the interaction or bonding between cations and anions, the framework formed by anions and their local configurations could all affect the ion transportation or diffusion to various degrees. There have been extensive attempts and efforts to gain a better understanding of the mechanism of the superionic conductivity in some sulphate crystals containing alkali metal cations. Among different models, the "paddle-wheel" mechanism mainly attributes the higher conductivity to the strong coupling between the rotational motions of SO_4 anions and cations and considers the radii of the cations of little importance for their diffusion rates [20–22,42]. According to this model, the rotating sulphate anions may push the cations and/or possibly lower potential thresholds making it easier for a vibrating ion to jump to an empty adjacent position [20]. In contrast, the percolation mechanism [43,44] emphasizes the role of cation radii and mass on the diffusion coefficients and it favours the idea that the diffusion of cation is enhanced by the lattice expansion and/or incorporation of ion vacancies by guest ion presence and the structural transition. This model considers that the contribution of the rotating SO_4 anions to the conductivity is not directly associated with its coupling with the cation (or the correlation is less important), but indirectly by the lowering of the potential thresholds, thus increasing the probability of a cation jumping to an empty adjacent position. Based on neutron diffraction measurements and reverse Monte Carlo modelling, Karlsson and McGreevy [23] have reported that the ionic conductivity in Li_2SO_4 and $LiNaSO_4$ is a combination of both paddle-wheel and percolation mechanisms. Results from quasielastic neutron scattering analysis have suggested that the anion reorientation and cation hopping have a similar time scale and time-of-flight experiments revealed both diffusional and reorientational contributions to the quasielastic scattering for $LiNaSO_4$ [45]. The work of Ferrario et al. [46] has indicated a more complex picture of the cation transport in lithium sulphate-based crystals and they considered contributions from lattice thermal vibrations, centre of mass displacement and reorientation of the sulphate groups.

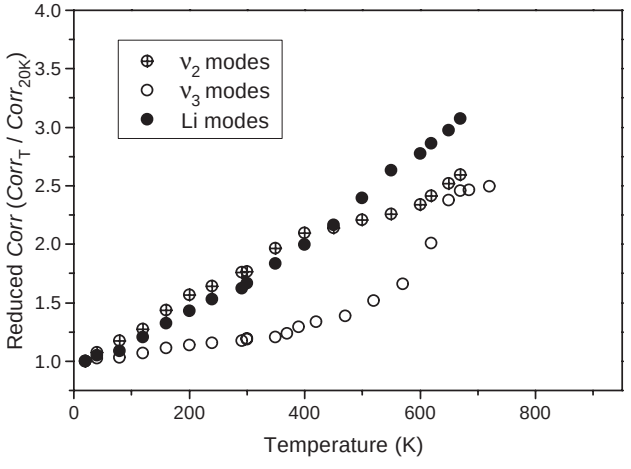

Fig. 7. Temperature dependence of reduced corr ($corr_T/corr_{20\ K}$).

As described earlier, the room-temperature reflectance spectrum of $LiNaSO_4$ shows a significant increase in reflectivity with decreasing wavenumber in the far-IR region. This is consistent with the reported, relatively high conductivity of $LiNaSO_4$. The data from the present study suggest that the conductivity of $LiNaSO_4$ may be associated with a complex combination of different contributions and they appear to play different roles in different temperature ranges. With increasing temperature, the dramatic changes occurring in the Li spectra indicate thermally induced Li site disordering and diffusion. The appearance of an additional Li mode near 380 cm^{-1} around 500 K is interesting. Our observation of the mode at temperatures as low as 500 K indicates that this mode is not the characteristic phonon mode required by the high-temperature (above 791 K) cubic structure of $LiNaSO_4$, but due to new

local sites for diffused Li or relaxational processes associated with cation mobility. This observation indicates that cation hopping does occur in $LiNaSO_4$ far below the phase transition temperature. The systematic increase in the intensity of the additional Li mode near 380 cm^{-1} (Fig. 4) further suggests that more Li atoms involve the process on heating. This cation diffusion may undoubtedly play a role in the conductivity. Although the trigonal–cubic phase transition is reported to take place near 791 K, the spectral changes of SO_4 modes occurring near 620 K (Figs. 6 and 7) indicate the onset of the SO_4 orientational disorder. The effect of increasing temperature is likely to facilitate or enhance the reorientational motion of the SO_4 group and the disorder, eventually leading to the breaking of the local symmetry associated with the ions and resulting in the dramatic change in the internal modes of SO_4. The observation is consistent with results from the high-temperature Raman measurements [16,47]. However, the results from the present study are fully consistent with the idea that Li and SO_4 strongly correlated during the SO_4 orientational disorder, although the transition surely affects the local configurations around the Li atoms and the conductivity. Although the v_2 modes showed similar variation as the Li bands (Fig. 7), the very different thermal behaviours between the Li mode and most of the internal modes (v_1, v_3 and v_4) of SO_4 appear to suggest that in the measured temperature range the two different types of ions react independently to the change of temperature. In fact, the Li bands do not show a significant change of its temperature dependence near 620 K where the onset of the SO_4 orientational disorder occurred and dramatic variations in the SO_4 spectra were recorded. This appears to suggest that the orientational disorder have only a weak effect on the behaviours of the Li atoms.

References

[1] B. Morosin, D.L. Smith, Acta Crystallographica 22 (1967) 906.
[2] T. Förland, J. Krong-Moe, Acta Crystallographica 11 (1958) 224.
[3] L. Nilsson, N.H. Andersen, A. Lundén, Solid Sate Ionics 34 (1989) 111.
[4] H.-C. Freiheit, Solid State Communications 119 (2001) 539.
[5] H.-C. Freiheit, H. Kroll, A. Putnis, Zeitschrift fur Kristallographie 213 (1998) 575.
[6] K. Singh, V.K. Deshipande, Solid Sate Ionics 13 (1984) 157.
[7] B.-E. Mellamder, G. Granéli, J. Roos, Solid Sate Ionics 40/41 (1990) 162.
[8] N. Bagdassarov, H.-C. Freiheit, A. Putnis, Solid State Ionics 143 (2001) 285.
[9] K.-D. Junke, M. Mali, J. Roos, D. Brinkmann, A. Lundén, B. Granénli, Solid Sate Ionics 28–30 (1988) 1287.
[10] D. Massiot, C. Bessada, P. Echegut, J.P. Coputures, Solid State Ionics 37 (1990) 223.
[11] T. Kanashiro, T. Yamanishi, Y. Kishimoto, T. Ohno, Y. Michihiro, K. Nobugai, Journal of the Physical Society of Japan 63 (1994) 3488.
[12] D. Teeters, R. Frech, Solid State Ionics 5 (1981) 437.
[13] D. Teeters, R. Frech, Journal of Chemical Physics 76 (1982) 799.
[14] D. Teeters, R. Frech, Physical Review. B 26 (1982) 4132.
[15] E.A. Secco, Journal of Chemical Physics 79 (1983) 5208.
[16] R. Frech, D. Teeters, Journal of Physical Chemistry 88 (1984) 417.
[17] M.A. Pimenta, P. Echegut, G. Hauret, F. Gervais, Phase Transitions 9 (1987) 185.
[18] K.-D. Junke, M. Mali, J. Roos, D. Brinkmann, Solid Sate Ionics 28–30 (1988) 1329.
[19] U.M. Gundusharma, C. MacLean, E.A. Secco, Solid State Communications 57 (1986) 479.
[20] A. Lundén, Solid State Communications 65 (1988) 1237.
[21] A. Lundén, Solid State Ionics 68 (1994) 77.
[22] N.H. Andersen, P.W.S.K. Bandaranayake, M.A. Careem, M.A.K.L. Dissanayake, C.N. Wijayasekera, R. Kaber, A. Lundén, B.-E. Mellander, L. Nilsson, J.O. Thomas, Solid State Ionics 57 (1992) 203.
[23] L. Karlsson, R.L. McGreevy, Solid State Ionics 76 (1995) 301.
[24] R. Tärneberg, A. Lundén, Solid State Ionics 90 (1996) 209.
[25] M. Zhang, B. Wruck, A. Graeme-Barbar, E.K.H. Salje, M.A. Carpenter, American Mineralogists 81 (1996) 92.
[26] M. Zhang, H.W. Meyer, L.A. Groat, U. Bismayer, E.K.H Salj, G. Adiwidjaja, Physics and Chemistry in Minerals 26 (1999) 546.
[27] Y. Yagil, F. Baudenbacher, M. Zhang, J.R. Birch, H. Kinder, E.K.H. Salje, Physical Review. B 52 (1995) 15582.
[28] M. Zhang, H. Xu, E.K.H. Salje, P.J. Heaney, Physics and Chemistry of Minerals 30 (2003) 457.
[29] P. Brüesh, Phonons: Theory and Experiments. II Experiments and Interpretation of Experimental Results, Springer-Verlag, 1986.
[30] J. Hiraishi, N. Taniguchi, H. Takahashi, Journal of Chemical Physics 65 (1976) 3821.
[31] G. Herzberg, Infrared and Raman Spectra of Polyatomic Molecules, Van Nostrand, New York, 1945.
[32] J. Petzelt, G.V. Kozlov, A.A. Volkov, Y. Ishibashi, Zeitschrift für Physik. B 33 (1979) 369.
[33] S.L. Chaplot, K.R. Rao, A.P. Roy, Physical Review. B 29 (1984) 4747.
[34] M. Zhang, E.K.H. Salje, A. Putnis, Journal of Physics. Condensed Matter 10 (1998) 11811.
[35] N.D. Zhigadlo, M. Zhang, E.K.H. Salje, Journal of Physics. Condensed Matter 13 (2001) 6551.
[36] D. Brinkmann, M. Mali, J. Roos, E. Schweickert, Solid State Ionics 5 (1981) 433.
[37] P. da R. Andrade, S.P.S. Porto, Solid State Communications 13 (1973) 1249.
[38] E.K.H. Salj, M.A. Carpenter, T.G.W. Malcherek, T. Boffa Ballaran, European Journal of Mineralogy 12 (2000) 503.
[39] W.H. Press, S.A. Teukolsky, V.T. Vetterlin, B.P. Flannery, Numerical Recipes in FORTRAN, Cambridge University Press, 1992.
[40] S.-B. Kim, R. Frech, Journal of Chemical Physics 88 (1988) 2216.
[41] S. Shin, Y. Tezuka, A. Sugawara, M. Ishigame, Physical Review. B 44 (1991) 11724.
[42] A. Kvist, A. Bengtzelius, in: W. van Gool (Ed.), Fast Ion Transport in Solids, North-Hlland, Amsterdam, 1973.
[43] E.A. Secco, Journal of Solid State Chemistry 96 (1992) 366.
[44] E.A. Secco, Solid Sate Ionics 60 (1993) 233.
[45] D. Wilmer, H. Feldmann, J. Combet, R.E. Lechner, Physica B 301 (2001) 99.
[46] M. Ferrario, M.L. Klein, I.R. McDonald, Molecular Physics 86 (1995) 923.
[47] G. Dharmasena, R. Frech, Journal of Chemical Physics 102 (1995) 6941.